Black paints covered with multidielectrics: light absorbers

G. SORIANO,* M. ZERRAD, [ID] AND C. AMRA [ID]

Aix Marseille Univ, CNRS, Centrale Marseille, Institut Fresnel, Marseille, France
*opex@osa.org

Abstract: Black paints are commonly used to provide broadband light absorbers in high-precision optics. We show how multidielectric coatings improve the performances of these absorbers. The coated rough paints still exhibit a quasi-lambertian diffuse reflection, but this scattering pattern can be reduced by several orders of magnitude, which strongly enhances absorption. Predictions are based on an exact electromagnetic theory of light scattering from arbitrary rough multilayers. Results are also compared to useful approximate theories.

1. Introduction

Light absorbers are commonly required to cancel or reduce parasitic light in optical systems [1–12]. In the field of high precision optics (of which micro-multiplexing devices and multiple channel micro-sensors are examples) their specifications have become severe since they are a major limitation to the isolation rates between communication or imaging channels. Typically absorption should be higher than 0.99 in a broad-band spectral region (covering visible and NIR wavelengths), and current efforts are today devoted to broaden this band while overpassing an absorption level of 0.999. Also, these performances should be maintained whatever the illumination incidence and polarization.

Different techniques [1–12] can be used to produce such devices, and surely the most classical is to coat a smooth (polished) absorbing substrate with dielectric anti-reflective layers. In this case the design of the multidielectric coating can be optimized and drives the absorber performance. Another technique consists in the nano-patterning of the absorbing surface. The result of this patterning can be seen as a transition gradient layer which acts as an antireflection layer and the index gradient drives the absorber performance. Plasmonic nano-particles were also introduced to produce light absorbers, and more recently metamaterials. In most cases (coating and nano-patterning), absorption occurs in the bulk of the substrates. In this context another technique [3,13] has also met great success since it does not require any absorbing substrate, which makes easier miniaturization or integration procedures. It consists in the coating of a dielectric substrate with the alternation of a few dielectric and metallic interferential layers; in this case absorption occurs within the bulk of the coating whose thickness is around a few wavelengths. The absorber performance is connected with the design of the metal/dielectric coating [14–18]. Generally speaking all these devices are produced on smooth substrates so that the non-absorbed light is reflected in the specular direction of reflection, while light scattering from the sample roughness is negligible.

As an alternative solution, black paints have also provided great help in the production of light absorbers [1,2,4,19,20]. The process is different in the sense that specular reflection is replaced by diffuse reflectance with a quasi-lambertian scattering, due to high substrate roughness and short correlation length. To a first approximation, absorption in these rough black paints slightly differs from the absorption of a smooth substrate with the same paint refractive index, unless the paint bulk micro-structure is specially designed to optimize absorption, which leads to complexity and high cost. Hence to improve the performance of black paints, one can think of a

solution where these paints are covered again with multidielectric stacks. Such procedure would confer new degrees of freedom in the optimization of the rough absorber.

However the key point with this alternative is to know whether optical coatings hold their interferential properties when they are deposited on arbitrary rough surfaces. Indeed such properties result from an interferential equilibrium of the stationary field in the stack, usually established for perfectly smooth and parallel surfaces [14–17]. As an illustration, the worst scenario would be the case where most of the incident light is scattered by the first rough surface (in contact with air), with the consequence of slight penetration in the stack and negligible weight of the interferential process. Notice that previous results were achieved [4] and concern the coating of black surfaces with a unique low-index quarter-wave layer. These results were successful and this proved that the specific single layer did not break the interferential equilibrium. However the absorber performance remained limited due to the simplicity of the coating (one layer), so that we here address the general question of a multilayer deposited on a rough surface, that is: to which extent can optical coatings hold their interferential properties when deposited on rough multilayers? If these properties were hold, then anti-reflective multilayers could be deposited on black paints and their design could be optimized to broaden the spectral region, increase the absorption and stabilize the variations with incidence and polarization. Notice here that optical coatings are a cornerstone technology with ever increasing design complexity and industrial applications. To recall the state of the art, optical thin films provide a large variety of optical functions (such as antireflective, beam splitters, mirrors, polarizers, dichroic and narrow-band filters) which may involve hundreds of layers with low absorption and scattering losses, compacity similar to bulk materials and high laser-induced damage threshold [14–17].

In order to address this problem of optical scattering from arbitrary rough multilayers, an electromagnetic theory must be chosen or developed. Obviously the results will depend on the distribution of heights and slopes of the initial paint surface. The first-order Small Perturbation Method (or first-order electromagnetic theory [21–24]) is a perfect tool for the modelization of slightly rough multilayers. It can cope with hundreds of layers and is directly invertible, for which reason it has been largely used in the optical coating community. In some rare situations it must be completed with higher order models [25]. Though this theory has allowed to emphasize the anti-scattering effect [26] at the origins of this multidielectric black paint absorber, it cannot be used anymore to quantify the absorber performances. Indeed the paint roughness is around one micro-meter and the scattering pattern is quasi-lambertian, so that an exact theory must be used.

Actually very few methods apply to the resonant domain [27,28] where roughness parameters are comparable to the illumination wavelength. The number of methods again decreases when the illuminated sample is a rough multilayer [29,30]. In this paper we present and use a boundary integral formalism for the electromagnetic wave scattering from rough multilayers [25]. This boundary integral system is well fitted for both smooth and rough surfaces. However as a numerical solution of the rigorous scattering problem, this approach is numerically demanding. For that reason the theory is implemented with the Method of Moments (MoM) for two-dimensional scattering (one variable surface topography) [31], and the rough multilayer is illuminated with a tapered wave (a Gaussian beam), under S- or P-polarization [27]. With this theoretical tool, we analyse the angular and spectral performances of light absorbers made with different multilayered antireflection coatings deposited on black paints. Applications may concern the fields of space and remote sensing, cosmetics, stationary and textiles, imaging in complex media, amongst others.

In section 2 we briefly present the theory, while section 3 is devoted to numerical calculation. Subsection 3.1 is devoted to a single layer antireflective (AR) coating, while in subsections 3.2 and 3.3 the complexity of the coating is increased to reach better performances. The relevance of approximate scattering wave theories on those very rough mutlilayers is investigated in section 4.

Conclusion is given in section 5 and recalls that all results may open the door to a new class of broad-band light absorbers.

2. Rough layer boundary integral formalism

We consider a three homogeneous media problem where the layer Ω_2 is bounded by two non-intersecting rough surfaces Σ_n with equations $z = z_n + h_n(\mathbf{r})$ for $n = 1, 2$ in the Cartesian coordinates (x, y, z), and denoting $(x, y) = \mathbf{r}$ (Fig. 1). It is assumed that the two boundaries don't overlap, that is $z_1 + h_1(\mathbf{r}) > z_2 + h_2(\mathbf{r})$ for all $\mathbf{r}$. The layer is enlightened from superstrate $\Omega_1 : z > z_1 + h_1(\mathbf{r})$ through interface Σ_1. Wavelength in vacuum is denoted λ_0, so that angular frequency is $\omega = 2\pi c / \lambda_0$. Surface Σ_2 interfaces the layer from substrate Ω_3. Electromagnetical parameters at wavelength λ_0 are denoted (ε_m, μ_m) with $m = 1$ in the superstrate, $m = 2$ in the layer and $m = 3$ in the substrate.
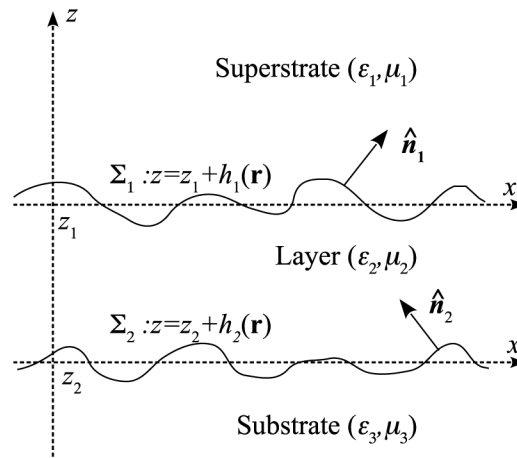

Fig. 1. Geometry of the problem

Assuming an $e^{-i\omega t}$ implicit time-dependency, the electromagnetic field $(\mathbf{E}, \mathbf{H})$ satisfies in domain Ω_m the time-harmonic Maxwell's equations $\mathbf{curl}\,\mathbf{E} = +i\omega\mu_m\mathbf{H}$ and $\mathbf{curl}\,\mathbf{H} = -i\omega\varepsilon_m\mathbf{E}$. The tangential components of the field $\hat{\mathbf{n}}_p \times \mathbf{E}$ and $\hat{\mathbf{n}}_p \times \mathbf{H}$ on both interfaces $p = 1, 2$ are continuous. $\hat{\mathbf{n}}_p$ denotes the unit normal vector, oriented from Ω_{p+1} toward Ω_p. This field also satisfies an outgoing wave condition in the substrate Ω_3. The incident field $(\mathbf{E}^{inc}, \mathbf{H}^{inc})$ satisfies the Maxwell's equations for $m = 1$: it writes as a sum of downward-directed plane waves

$$\mathbf{E}^{inc}(\mathbf{r}, z) = \int_{\mathbb{R}^2} \mathbf{E}_1^{0-}(\mathbf{k}) e^{i(\mathbf{k}\cdot\mathbf{r} - q_1 z)} d\mathbf{k} \tag{1}$$

with $k^2 + q_1^2 = \omega^2\varepsilon_1\mu_1$ and $0 \le \arg q_1 \le \pi/2$. The scattered field $(\mathbf{E} - \mathbf{E}^{inc}, \mathbf{H} - \mathbf{H}^{inc})$ satisfies an outgoing wave condition in the superstrate.

The reference field $(\mathbf{E}^0, \mathbf{H}^0)$ corresponds to the field $(\mathbf{E}, \mathbf{H})$ in the case where the layer surfaces are two parallel planes $z = z_1$ and $z = z_2$. The plane waves expansion of the reference field in the three media write

$$\int_{\mathbb{R}^2} \left\{ \mathbf{E}_m^{0+}(\mathbf{k}) e^{i(\mathbf{k}\cdot\mathbf{r} + q_m z)} + \mathbf{E}_m^{0-}(\mathbf{k}) e^{i(\mathbf{k}\cdot\mathbf{r} - q_m z)} \right\} d\mathbf{k} = \mathbf{E}_m^0(\mathbf{r}, z) \tag{2}$$

with $k^2 + q_m^2 = \omega^2\varepsilon_m\mu_m$ and $0 \le \arg q_m \le \pi/2$. Outgoing wave condition in the substrate leads to $E_3^{0+}(\mathbf{k}) = \mathbf{0}$ for all $\mathbf{k}$. In Eq. (2), those three plane wave expansions are extended to the whole space to define the three fields $(\mathbf{E}_m^0, \mathbf{H}_m^0)$.

Now, for rough interfaces, the tangential components of the field $\hat{\mathbf{n}}_p \times \mathbf{E}$ and $\hat{\mathbf{n}}_p \times \mathbf{H}$, cast into the vector form

$$X = \begin{bmatrix} \hat{\mathbf{n}}_1 \times \mathbf{E} \\ \hat{\mathbf{n}}_1 \times \mathbf{H} \\ \hat{\mathbf{n}}_2 \times \mathbf{E} \\ \hat{\mathbf{n}}_2 \times \mathbf{H} \end{bmatrix} \tag{3}$$

satisfy the linear system

$$A(X - Y) = C(Z - Y) \tag{4}$$

of coupled boundary integral equations. The two vectors

$$Y = \begin{bmatrix} \hat{\mathbf{n}}_1 \times \mathbf{E}_1^0 \\ \hat{\mathbf{n}}_1 \times \mathbf{H}_1^0 \\ \hat{\mathbf{n}}_2 \times \mathbf{E}_2^0 \\ \hat{\mathbf{n}}_2 \times \mathbf{H}_2^0 \end{bmatrix} \qquad Z = \begin{bmatrix} \hat{\mathbf{n}}_1 \times \mathbf{E}_2^0 \\ \hat{\mathbf{n}}_1 \times \mathbf{H}_2^0 \\ \hat{\mathbf{n}}_2 \times \mathbf{E}_3^0 \\ \hat{\mathbf{n}}_2 \times \mathbf{H}_3^0 \end{bmatrix} \tag{5}$$

are determined from the reference field on the rough boundaries. Matrix A writes

$$A = \begin{bmatrix} \frac{1}{2} - \mathcal{K}_1^{11} & -\mu_1 \mathcal{T}_1^{11} & 0 & 0 \\ \frac{1}{2} + \mathcal{K}_2^{11} & +\mu_2 \mathcal{T}_2^{11} & -\mathcal{K}_2^{12} & -\mu_2 \mathcal{T}_2^{12} \\ +\mathcal{K}_2^{21} & +\mu_2 \mathcal{T}_2^{21} & \frac{1}{2} - \mathcal{K}_2^{22} & -\mu_2 \mathcal{T}_2^{22} \\ 0 & 0 & \frac{1}{2} + \mathcal{K}_3^{22} & +\mu_3 \mathcal{T}_3^{22} \end{bmatrix} \tag{6}$$

introducing (notations are derived from [32] and generalized to layered media) the EFIE operator

$$\mathcal{T}_m^{np} \mathbf{j}(\mathbf{R}_n) = \hat{\mathbf{n}}_n \times \int_{\Sigma_p} i\omega \, \bar{\mathrm{G}}_m(\mathbf{R}_n - \mathbf{R}_p) \cdot \mathbf{j}(\mathbf{R}_p) dS_p \tag{7}$$

and the MFIE operator

$$\mathcal{K}_m^{np} \mathbf{j}(\mathbf{R}_n) = \hat{\mathbf{n}}_n \times \int_{\Sigma_p} \mathbf{curl} \, \bar{\mathrm{G}}_m(\mathbf{R}_n - \mathbf{R}_p) \cdot \mathbf{j}(\mathbf{R}_p) dS_p \tag{8}$$

with $\mathbf{j}$ a tangential vector field and for two point $\mathbf{R}_n$ and $\mathbf{R}_p$ on interfaces Σ_n and Σ_p, respectively. Those operators involve the free space dyadic Green's functions $\bar{\mathbf{G}}_m(\mathbf{R}) = (\bar{\mathbf{I}} + K_m^{-2}\mathbf{grad}\,\mathrm{div})G_m(\mathbf{R})$. For passive media $m = 1, 2, 3$, the wavenumbers K_m satisfy $K_m^2 = (2\pi/\lambda)^2 \varepsilon_m \mu_m$ with $0 \le \arg K_m \le \pi/2$. The scalar Green's functions are driven by equations $(\mathrm{div}\,\mathbf{grad} - K_m^2)G_m(\mathbf{R}) = -\delta(\mathbf{R})$ and radiation condition. Matrix C

$$C = \begin{bmatrix} 0 & 0 & 0 & 0 \\ \frac{1}{2} + \mathcal{K}_2^{11} & +\mu_2 \mathcal{T}_2^{11} & 0 & 0 \\ +\mathcal{K}_2^{21} & +\mu_2 \mathcal{T}_2^{21} & 0 & 0 \\ 0 & 0 & \frac{1}{2} + \mathcal{K}_3^{22} & +\mu_3 \mathcal{T}_3^{22} \end{bmatrix} \tag{9}$$

is a sparsified version of matrix A. Such a theory can easily be extended to structures with an arbitrary number of layers.

Then, the scattered electric field writes in the $z > z_1 + \max h_1$ region of the superstrate as the sum of plane waves:

$$(\mathbf{E} - \mathbf{E}^{inc})(\mathbf{r}, z) = \int_{\mathbb{R}^2} \mathbf{E}^+(\mathbf{k}) e^{i(\mathbf{k} \cdot \mathbf{r} + q_1 z)} d\mathbf{k} \tag{10}$$

Their amplitude is related to the tangential components of the fields on Σ_1 through expression:

$$\mathbf{E}^+(\mathbf{k}) = +\frac{\mathbf{K}_1}{8\pi^2 q_1} \times \int_{\Sigma_1} \left\{ \frac{\mathbf{K}_1}{\omega \varepsilon_1} \times (\hat{\mathbf{n}}_1 \times \mathbf{H}) - \hat{\mathbf{n}}_1 \times \mathbf{E} \right\} e^{-i\mathbf{K}_1 \cdot \mathbf{R}_1} dS_1 \tag{11}$$

with $\mathbf{K}_1 = \mathbf{k} + q_1 \hat{\mathbf{z}}$ the upward-directed wavevector.

Finally, this electric field formulation is turned into a magnetic field formulation by substituing $\mathbf{E} \leftrightarrow \mathbf{H}$ and $\mu \leftrightarrow -\varepsilon$ in Eqs. (1)–(6) and (9)–(11).

3. Numerical calculation

In the next sections the substrate roughness is assumed to be normally distributed with a gaussian spectrum of correlation length $L_g = 1 \, \mu$m. The roughness root mean square (rms) height is $\delta = 250$ nm, so that the rms slope is $s = 0.353$ and the inverse rms curvature [33] is $\gamma = 1.31 \, \mu$m. These values correspond to what can be typically measured on rough surfaces with near-field microscopy [34]. We also consider that the height profiles are fully correlated from one interface to another, as a general result issued from modern thin film deposition technologies (Ion Assisted Deposition, Dual Ion Beam Sputtering, Magnetron Sputtering to name only the most common) which are known to replicate the substrate roughness throughout a multilayer [23,24].

Numerical calculation is performed for wavelengths in the range (400 nm - 1 μm), while the scattering angles vary between $0°$ and $90°$ in the half space of the incident and reflected beams. The illumination beam is a Gaussian beam centered on normal incidence $i = 0°$ and with beam divergence $\Delta i = 1.5°$. The coatings involve two dielectric thin film materials with high (n_H) and low (n_L) refraction indices. Indeed most optical interferential functions can be designed with two materials (even though more materials could be used), which provide the simplest solution, all the more that these solutions simplify the vacuum deposition process and the in-situ thickness monitoring. In this paper, these two materials are tantalum pentoxide (Ta2O5) and silicon dioxide (SiO2) with refraction indices $n_H = 2.130$ and $n_L = 1.489$, respectively, at the wavelength $\lambda = 633$ nm. This couple of materials Ta2O5/SiO2 has been commonly used these last decades for applications in the visible, though it can be replaced today by Nb2O5/SiO2.

The incident medium is air ($n_0 = 1.000$) and the substrate index is that of the black paint ($n_s = 1.750$). Note that this last index was measured in a previous paper [4] on the basis of TIS (Total Integrated Scattering) data measured before and after coating the paint. The imaginary part of the paint index is below 0.1% and does not impact the free space scattering pattern in air, so that its exact knowledge is not required. On the other hand, this imaginary index guarantees that light is absorbed within the paint.

The Method of Moments detailed in section 2 is a deterministic method, so that statistical results are obtained through a Monte Carlo average over 256 realizations.

3.1. Single layer AR coating

In this section we start with a single low-index (SiO2) quarter-wave layer since this was the original idea resulting from the anti-scattering effect [26]. Hence the design is denoted as Air/L/Black Paint, where L indicates the quarter-wave optical thickness at the design wavelength $\lambda_0 = 633$ nm. Results are given in Fig. 2 for the angular scattering pattern calculated at an illumination wavelength λ equal to the design wavelength λ_0. In this figure the blue curve (labeled S0) is plotted for the scattering pattern of the uncoated black paint. We first observe the lambertian behaviour of this pattern, which is characteristic of a short roughness to correlation

length ratio. The normalized angular scattering level, defined as the reflected and scattered power per degree of scattering angle and per unit of incident power, is around $4.3 \cdot 10^{-2}$ at low angles, and the total scattering (integrated over all angles) is 8.2% for S-polarization and 6.5% for P-polarization. Hence the absorption of the bare paint is A_S = 91.8% for S-polarization and A_P = 93.5% for P-polarization.
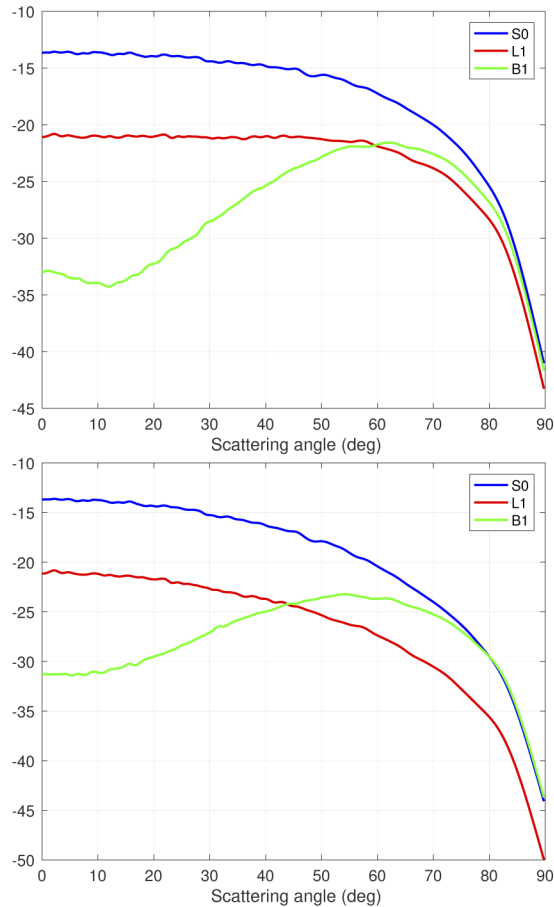

Fig. 2. Angular scattering pattern at 633nm from the rough black paint, before (S0) and after (L1, B1) coating by a single (L1) or double (B1) anti-reflecting coating. S and P polarizations are considered (top and bottom figures respectively)

In the same Fig. 2 the red curve (labeled L1) is plotted for the paint coated with the quarter-wave layer. We observe a strong reduction of scattering (by a factor 5.5), so that the resulting absorption is increased up to A_S = 98.1% and A_P = 98.9%. This result proves that interferences still occur for the coating deposited on the rough surface, at least for a single low-index layer.

3.2. Increasing the absorption with a double-layer AR coating

Now that this simple coating was shown to hold its antireflective properties, one can try to propose more complex stacks in order to increase the absorption. Indeed the previous AR coating does not allow to cancel (but reduces) specular reflection at λ_0, due to the fact that the layer index n_L does not satisfy the ideal AR relationship n_L = 1.489 $\neq \sqrt{n_0 n_s}$ = 1.323. So we can expect better performances if we use a double layer AR coating which totally cancels the specular

reflection (at least for normal illumination) at λ_0. For that we consider the following design [14] involving two materials, that is: Air / 0.672L/1.645H / Black Paint.

Such design means that, at the design wavelength $\lambda_0 = 633$ nm, the optical thickness of the low-index layer is $0.672\lambda_0/4$, while that of the high-index is 1.645. Results are plotted again in Fig. 2 (green curve, labelled B1) and show a stronger reduction of scattering, by a factor 10 at low angles. The normalized total integrated scattering is $9 \cdot 10^{-3}$ for S-polarization, which gives an absorption $A_S = 99.1\%$, while this same quantity reaches $A_P = 99.3\%$ for P-polarization. Hence these results are highly successful if monochromatic properties are considered.

At this step it is interesting to emphasize the connection between the specular properties of the coating and those of scattering. This is shown in Fig. 3 where are plotted the angular variations $R(i)$ of the reflection coefficients of the same single and double AR coatings deposited on a smooth (not rough) paint. In this figure, we observe that at low illumination angles, the lower the reflection, the lower the scattering. In other words, the weight of scattering is driven by the reflection coefficient of the AR stack. We also observe that this result fails at large angles.
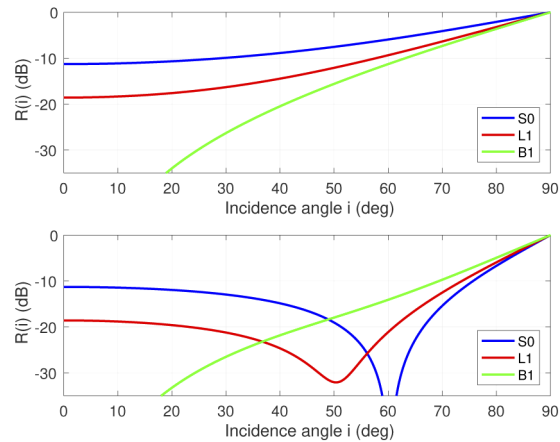

Fig. 3. Specular reflection R(i) of the ideally smooth substrate and the AR coatings of Fig. 2, plotted versus the illumination incidence i. Case of S and P polarizations (top and bottom figures respectively).

Eventually one cannot forget that these components are also required to absorb light in a broad-band region of wavelengths. For that reason their spectral performances are also plotted in Fig. 4. In this figure the vertical data are those of the absorption, averaged over both polarizations. As expected, the double AR coating (green curve, labeled B1) shows higher efficiency but in a narrower band of wavelengths. Note that optical index dispersion of the black paint and thin film materials are here neglected.

As was done for the illumination incidence, we also plotted in Fig. 5 the specular properties of the single and double AR coatings (deposited on a smooth substrate) versus wavelength. The results again emphasize the key role of the coatings in the absorber performances.

3.3. Broadening the spectral band with a four-layer antireflective coating

One last attempt consists in broadening the spectral band with more complex structures. For that we use a 4-layer broadband AR coating whose design is: Air / L 17.039 nm / H 35.761 nm / L 20.072 nm / H 101.278 nm / Black Paint.

For this structure, the optical index dispersion of the thin film materials is taken into account, as shown on Table 1. Those index values are issued from Perkin Elmer Lambda 1050 spectrophotometer measurements in our laboratory.
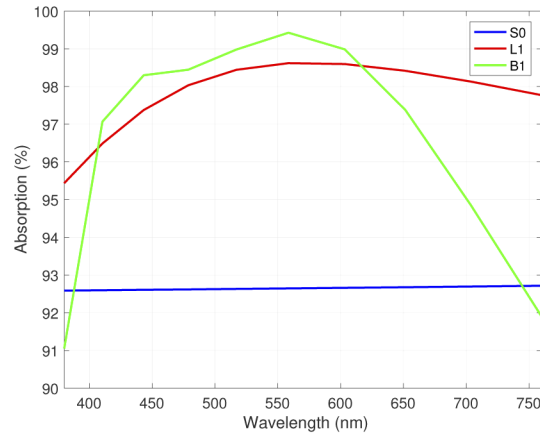
Fig. 4. Absorption versus wavelength for the rough substrate and the AR coatings of Fig. 2.
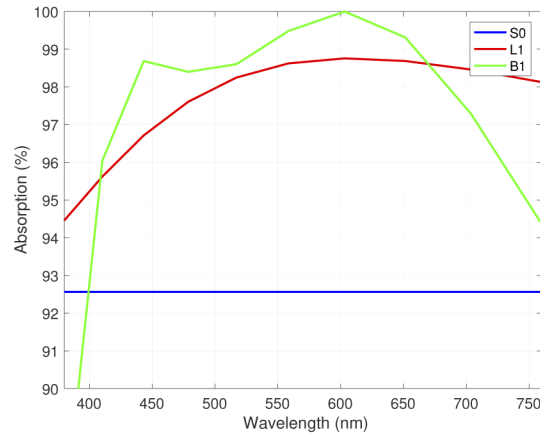

Fig. 5. Absorption versus wavelength for the ideally smooth substrate and single and double AR coatings.

Table 1. Optical indices at visible wavelengths for the 4-layer broad band AR coating.

λ (nm)	n'_L	n''_L	n'_H	n''_H
380.0	1.496	1.056e-04	2.605	1.607e-04
410.4	1.492	5.822e-05	2.525	1.968e-04
443.3	1.488	3.353e-05	2.464	2.812e-05
478.8	1.486	2.012e-05	2.417	4.641e-06
517.1	1.483	1.253e-05	2.381	8.754e-07
558.5	1.481	8.090e-06	2.353	1.868e-07
603.2	1.479	5.393e-06	2.332	4.472e-08
651.5	1.478	3.705e-06	2.315	1.187e-08
703.7	1.477	2.617e-06	2.302	3.517e-09
760.0	1.476	1.897e-06	2.292	1.1e-09

Following the previous results, one can expect that the absorber performances will follow those of this broad-band AR design which are shown in Fig. 6 (red curve for case of smooth surfaces). This is indeed what we observe, that is an absorption level greater than 97% over the whole band (400nm-700nm). Hence these successful results open the door to more complex designs for the future.
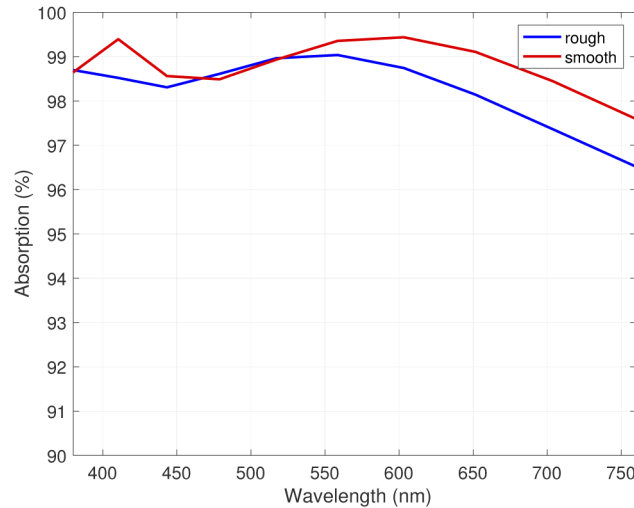

Fig. 6. Spectral absorption on the 400 nm-1 μm band for a rough black paint covered with the four-layers F4 coating (blue curve) and for the ideally smooth 4-layer broad-band AR coating (red curve).

4. Approximate scattering wave theories

Fast and approximate calculation may be of great help in the analysis of light scattering from rough multilayers, and provide meaningful information for the design of such advanced coatings. For that reason, rigorous (MoM) computations of the scattered field by the bare black painting S0, the single-layer coating L1 and the double-layers coating were compared to several approximate scattering wave theories [35].

The two asymptotic methods, that are the first-order small perturbation method (SPM1) in the low-frequency limit [21–24] and the geometrical optics theory (GO) in the high-frequency limit [36,37], were tested. With a rms height to wavelength ratio of $\delta/\lambda = 0.4$, the SPM1 is far from its validity domain (which definition varies in the literature from $\delta/\lambda < 1/10$ to $\delta/\lambda < 1/50$), and was indeed found irrelevant. The classical validity criterion for high-frequency approximations is $(2\pi/\lambda)\gamma \cos^3\theta \gg 1$. For the rough black paint, we have $(2\pi/\lambda)\gamma = 13$, and the criterion is fulfilled, in that sense that $(2\pi/\lambda)\gamma \cos^3\theta > 1$, up to a scattering angle of $\theta = 65°$.

For rough multilayers with perfectly correlated interfaces, the generalization of GO from single interface is rather straightforward. The smooth multilayer reflection coefficient is computed for a local angle of $\theta/2$ that matches a specular configuration for normal illumination. The scattering level is then made proportional to the probability for the rough multilayer slope to equal $-\tan^{-1}(\theta/2)$. The slope is normally distributed, since the rough multilayer height is assumed to be.

GO simulations are added in dashed lines to the MoM on Fig. 7. For the bare rough paint (blue curves), the GO remarkably fits the MoM within the Monte Carlo process uncertainty small and intermediate angles up to 60°, which is in accordance with the GO validity domain determined earlier. This applies for both polarizations. Beyond that angle, the GO fails to tend toward zero;

this is a well-know flaw of the method. Shadowing models [38] might be of some help here. Results for the single layer AR coating (red curves of Fig. 7) are quite similar, except that GO and MoM split at a smaller angle around 40°. Beyond this angle and up to 75° in S-polarization (and 85° in P-polarization), GO underestimates the scattering level but with an error smaller than 2dB. The analysis of the results for the double layer AR coating (green curves of Fig. 7) is much worse: the global shape of the scattering diagram is not retrieved by the GO. On the 0° − 60° angular range, the GO scattering level is always 10dB lower than the MoM. The analytic zero level of the smooth multilayer reflection coefficient at normal incidence is too strongly passed on the GO, while multiple scattering that is taken into account by the MoM transforms this zero level into a smooth minimum (Fig. 7). This last feature, that in out opinion shall be met with any single-scattering wave theory [35], is in accordance with similar results recently shown [25] when analyzing with exact theories on low-roughness surfaces, the performance of the antiscattering effect [26].
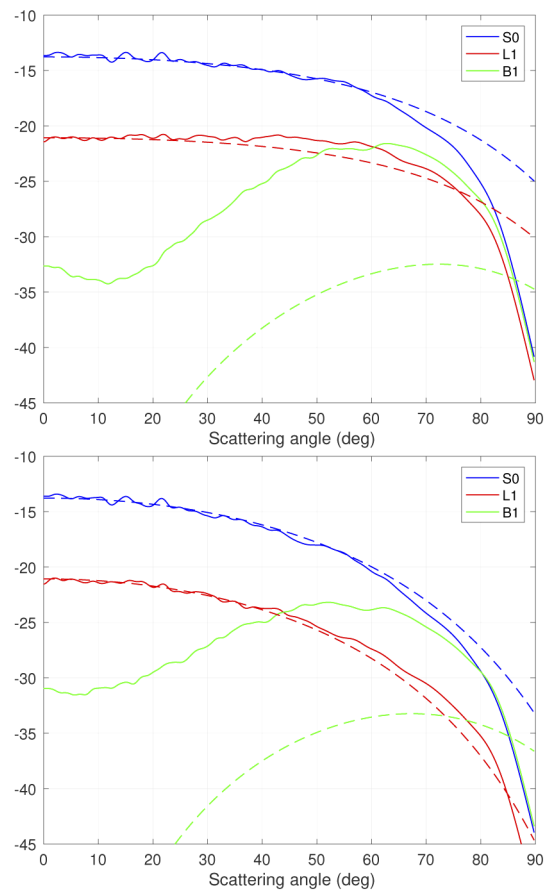

Fig. 7. Angular scattering patterns at 633nm of Fig. 2 compared to GO (dashed lines).

To summarize, we can state that even for rough multilayers, a useful approximation will often be provided by the GO model. However one has to keep in mind that this approximation will fail in situations where the optical properties of the stack (at the working wavelength) rely on a highly sensitive interferential balance driven by destructive interferences between waves scattered from the rough interfaces. Namely, this concerns high-performance antireflective coatings and narrow-band filters.

5.   Conclusion

Using an exact electromagnetic theory of light scattering from arbitrarily rough surfaces, we have shown that multilayer AR optical coatings hold their interferential properties when deposited on rough surfaces which scatter light in a lambertian way. Such property opens the door to enhanced broad-band light absorbers which can be produced with the state of the art multilayer AR designs deposited on black paints. Other applications may concern cosmetics and stationery, lightning and textiles, remote sensing (bio-mass), living and vegetal tissues. Future work will include experiments which consist in coating and measuring different paints with thin film materials (oxydes) and deposition technologies (Ion Beam Sputtering, Ion Assisted Deposition, Magnetron Sputtering) that are available at Institut Fresnel (RCMO group).

It would be interesting to emphasize the rms slope limit above which rough optical coatings loose their interferential properties. The same limit should be analyzed versus the number of layers, and versus the surfaces cross-correlation functions which may depend on the deposition technology. The implementation of the theory is however computationally demanding with a heavy burden on memory, and this does not allow to answer these questions at this step. Work is in progress. Note also that this work should be completed with a variety of black paints whose indices should be first measured using the same techniques. Indeed the average of the angular scattering pattern is not highly sensitive to the details of the surface topography. For this reason, the paint index can be extracted from the modification of the scattering pattern after deposition of a coating which is known.

To conclude, we would like to stress with an analogy of coatings deposited on microspheres. In previous works [39] we analyzed the spectral properties of coatings deposited on microspheres. Depending on the sphere diameters and the coating design, it was shown that the interferential properties could be hold. Typically, with a 7 layer multidielectric mirror, the global behaviour of the spectral profile was nearly maintained, with diameters around a few micrometers. This positively compares with the inverse rms curvature ($1.3\ \mu$m) of the surfaces under study in this paper (section 3).

Funding

Acknowledgments

Disclosures

The authors declare no conflicts of interest.

References

1. C. Andrews, "Thin black screens for diffraction measurements," J. Opt. Soc. Am. **58**(7), 941–945 (1968).
2. W. Blevin and J. Geist, "Influence of black coatings on pyroelectric detectors," Appl. Opt. **13**(5), 1171–1178 (1974).
3. M. Cathelinaud, F. Lemarquis, and C. Amra, "Index determination of opaque and semitransparent metallic films: application to light absorbers," Appl. Opt. **41**(13), 2546–2554 (2002).
4. H. Giovannini and C. Amra, "Dielectric thin films for maximized absorption with standard quality black surfaces," Appl. Opt. **37**(1), 103–105 (1998).
5. S. Zhang, Y. Li, G. Feng, B. Zhu, S. Xiao, L. Zhou, and L. Zhao, "Strong infrared absorber: surface-microstructured au film replicated from black silicon," Opt. Express **19**(21), 20462–20467 (2011).
6. Z. Liu, P. Zhan, J. Chen, C. Tang, Z. Yan, Z. Chen, and Z. Wang, "Dual broadband near-infrared perfect absorber based on a hybrid plasmonic-photonic microstructure," Opt. Express **21**(3), 3021–3030 (2013).
7. J. Sun, L. Liu, G. Dong, and J. Zhou, "An extremely broad band metamaterial absorber based on destructive interference," Opt. Express **19**(22), 21155–21162 (2011).

8. L. Lei, S. Li, H. Huang, K. Tao, and P. Xu, "Ultra-broadband absorber from visible to near-infrared using plasmonic metamaterial," Opt. Express **26**(5), 5686–5693 (2018).
9. J. Chen, Y. Jin, P. Chen, Y. Shan, J. Xu, F. Kong, and J. Shao, "Polarization-independent almost-perfect absorber controlled from narrowband to broadband," Opt. Express **25**(12), 13916–13922 (2017).
10. N. I. Landy, S. Sajuyigbe, J. J. Mock, D. R. Smith, and W. J. Padilla, "Perfect metamaterial absorber," Phys. Rev. Lett. **100**(20), 207402 (2008).
11. A. S. Rana, M. Zubair, M. S. Anwar, M. Saleem, and M. Q. Mehmood, "Engineering the absorption spectra of thin film multilayer absorbers for enhanced color purity in cmy color filters," Opt. Mater. Express **10**(2), 268–281 (2020).
12. M. K. Gunde and Z. C. Orel, "Absorption and scattering of light by pigment particles in solar-absorbing paints," Appl. Opt. **39**(4), 622–628 (2000).
13. F. Lemarquis and G. Marchand, "Analytical achromatic design of metal–dielectric absorbers," Appl. Opt. **38**(22), 4876–4884 (1999).
14. H. A. Macleod and H. A. Macleod, *Thin-film optical filters* (CRC, 2010).
15. A. Thelen, *Design of optical interference coatings* (McGraw-Hill Companies, 1989).
16. S. A. Furman and A. Tikhonravov, *Basics of optics of multilayer systems* (Atlantica Séguier Frontieres, 1992).
17. P. Baumeister, *Optical coating technology*, vol. 137 (SPIE, 2004).
18. F. Lemarquis, T. Begou, A. Moreau, and J. Lumeau, "Broadband antireflection coatings for visible and infrared ranges," CEAS Space J. **11**(4), 567–578 (2019).
19. A. B. Krewinghaus, "Infrared reflectance of paints," Appl. Opt. **8**(4), 807–812 (1969).
20. H. J. Basheer, C. Pachot, U. Lafont, X. Devaux, and N. Bahlawane, "Low-temperature thermal cvd of superblack carbon nanotube coatings," Adv. Mater. Interfaces **4**(18), 1700238 (2017).
21. J. Elson, J. P. Rahn, and J. Bennett, "Light scattering from multilayer optics: comparison of theory and experiment," Appl. Opt. **19**(5), 669–679 (1980).
22. J. Elson, J. Rahn, and J. Bennett, "Relationship of the total integrated scattering from multilayer-coated optics to angle of incidence, polarization, correlation length, and roughness cross-correlation properties," Appl. Opt. **22**(20), 3207–3219 (1983).
23. C. Amra, "Light scattering from multilayer optics. i. tools of investigation," J. Opt. Soc. Am. A **11**(1), 197–210 (1994).
24. C. Amra, "Light scattering from multilayer optics. ii. application to experiment," J. Opt. Soc. Am. A **11**(1), 211–226 (1994).
25. G. Soriano, M. Zerrad, and C. Amra, "Anti-scattering effect analyzed with an exact theory of light scattering from rough multilayers," Opt. Lett. **44**(18), 4455–4458 (2019).
26. C. Amra, G. Albrand, and P. Roche, "Theory and application of antiscattering single layers: antiscattering antireflection coatings," Appl. Opt. **25**(16), 2695–2702 (1986).
27. L. Tsang, J. A. Kong, K. H. Ding, and C. O. Ao, *Scattering of electromagnetic waves: numerical simulations*, Wiley series in remote sensing (Wiley-Interscience, 2001).
28. W. Chew, M. Tong, and B. Hu, *Integral Equation Methods for Electromagnetic and Elastic Waves* (Morgan & Claypool, 2008).
29. C.-H. Kuo and M. Moghaddam, "Scattering from multilayer rough surfaces based on the extended boundary condition method and truncated singular value decomposition," IEEE Trans. on Antennas Propag. **54**(10), 2917–2929 (2006).
30. M. Sanamzadeh, L. Tsang, and J. T. Johnson, "3-d electromagnetic scattering from multilayer dielectric media with 2-d random rough interfaces using *t*-matrix approach," IEEE Trans. on Antennas and Propagation **67**(1), 495–503 (2018).
31. G. Soriano, P. Spiga, and M. Saillard, "Low-grazing angles scattering of electromagnetic waves from one-dimensional natural surfaces: Rigorous and approximate theories," C. R. Phys. **11**(1), 77–86 (2010).
32. G. Hsiao and R. Kleinman, "Mathematical foundations for error estimation in numerical solutions of integral equations in electromagnetics," IEEE Trans. on Antennas Propag. **45**(3), 316–328 (1997).
33. J. A. Ogilvy, *Theory of Wave Scattering from Random Rough Surfaces* (Adam Hilger, 1991).
34. M. Zerrad, C. Deumie, M. Lequime, and C. Amra, "An alternative scattering method to characterize surface roughness from transparent substrates," Opt. Express **15**(15), 9222–9231 (2007).
35. T. Elfouhaily and C. A. Guérin, "A critical survey of approximate scattering wave theories from random rough surfaces," Waves Random Media **14**(4), R1–R40 (2004).
36. P. Beckmann and A. Spizzichino, *The scattering of electromagnetic waves from rough surfaces*, International series of monographs on electromagnetic waves (Pergamon, 1963).
37. F. Bass and I. Fuks, *Wave scattering from statistically rough surfaces*, International Series on Natural Philosophy **93** (Pergamon, 1979).
38. C. Bourlier, G. Berginc, and J. Saillard, "One-and two-dimensional shadowing functions for any height and slope stationary uncorrelated surface in the monostatic and bistatic configurations," IEEE Trans. on Antennas Propag. **50**(3), 312–324 (2002).
39. P. Voarino, C. Deumie, and C. Amra, "Optical properties calculated for multidielectric quarter-wave coatings on microspheres," Opt. Express **12**(19), 4476–4482 (2004).